Observation of the Semileptonic D^+ Decay into the $\bar{K}_1(1270)^0$ Axial-Vector Meson

M. Ablikim,[1] M. N. Achasov,[10,d] P. Adlarson,[59] S. Ahmed,[15] M. Albrecht,[4] M. Alekseev,[58a,58c] A. Amoroso,[58a,58c] F. F. An,[1] Q. An,[55,43] Y. Bai,[42] O. Bakina,[27] R. Baldini Ferroli,[23a] I. Balossino,[24a] Y. Ban,[35] K. Begzsuren,[25] J. V. Bennett,[5] N. Berger,[26] M. Bertani,[23a] D. Bettoni,[24a] F. Bianchi,[58a,58c] J. Biernat,[59] J. Bloms,[52] I. Boyko,[27] R. A. Briere,[5] H. Cai,[60] X. Cai,[1,43] A. Calcaterra,[23a] G. F. Cao,[1,47] N. Cao,[1,47] S. A. Cetin,[46b] J. Chai,[58c] J. F. Chang,[1,43] W. L. Chang,[1,47] G. Chelkov,[27,b,c] D. Y. Chen,[6] G. Chen,[1] H. S. Chen,[1,47] J. C. Chen,[1] M. L. Chen,[1,43] S. J. Chen,[33] Y. B. Chen,[1,43] W. Cheng,[58c] G. Cibinetto,[24a] F. Cossio,[58c] X. F. Cui,[34] H. L. Dai,[1,43] J. P. Dai,[38,h] X. C. Dai,[1,47] A. Dbeyssi,[15] D. Dedovich,[27] Z. Y. Deng,[1] A. Denig,[26] I. Denysenko,[27] M. Destefanis,[58a,58c] F. De Mori,[58a,58c] Y. Ding,[31] C. Dong,[34] J. Dong,[1,43] L. Y. Dong,[1,47] M. Y. Dong,[1,43,47] Z. L. Dou,[33] S. X. Du,[63] J. Z. Fan,[45] J. Fang,[1,43] S. S. Fang,[1,47] Y. Fang,[1] R. Farinelli,[24a,24b] L. Fava,[58b,58c] F. Feldbauer,[4] G. Felici,[23a] C. Q. Feng,[55,43] M. Fritsch,[4] C. D. Fu,[1] Y. Fu,[1] Q. Gao,[1] X. L. Gao,[55,43] Y. Gao,[45] Y. Gao,[56] Y. G. Gao,[6] Z. Gao,[55,43] B. Garillon,[26] I. Garzia,[24a] E. M. Gersabeck,[50] A. Gilman,[51] K. Goetzen,[11] L. Gong,[34] W. X. Gong,[1,43] W. Gradl,[26] M. Greco,[58a,58c] L. M. Gu,[33] M. H. Gu,[1,43] S. Gu,[2] Y. T. Gu,[13] A. Q. Guo,[22] L. B. Guo,[32] R. P. Guo,[36] Y. P. Guo,[26] A. Guskov,[27] S. Han,[60] X. Q. Hao,[16] F. A. Harris,[48] K. L. He,[1,47] F. H. Heinsius,[4] T. Held,[4] Y. K. Heng,[1,43,47] M. Himmelreich,[11,g] Y. R. Hou,[47] Z. L. Hou,[1] H. M. Hu,[1,47] J. F. Hu,[38,h] T. Hu,[1,43,47] Y. Hu,[1] G. S. Huang,[55,43] J. S. Huang,[16] X. T. Huang,[37] X. Z. Huang,[33] N. Huesken,[52] T. Hussain,[57] W. Ikegami Andersson,[59] W. Imoehl,[22] M. Irshad,[55,43] Q. Ji,[1] Q. P. Ji,[16] X. B. Ji,[1,47] X. L. Ji,[1,43] H. L. Jiang,[37] X. S. Jiang,[1,43,47] X. Y. Jiang,[34] J. B. Jiao,[37] Z. Jiao,[18] D. P. Jin,[1,43,47] S. Jin,[33] Y. Jin,[49] T. Johansson,[59] N. Kalantar-Nayestanaki,[29] X. S. Kang,[31] R. Kappert,[29] M. Kavatsyuk,[29] B. C. Ke,[1] I. K. Keshk,[4] A. Khoukaz,[52] P. Kiese,[26] R. Kiuchi,[1] R. Kliemt,[11] L. Koch,[28] O. B. Kolcu,[46b,f] B. Kopf,[4] M. Kuemmel,[4] M. Kuessner,[4] A. Kupsc,[59] M. Kurth,[1] M. G. Kurth,[1,47] W. Kühn,[28] J. S. Lange,[28] P. Larin,[15] L. Lavezzi,[58c] H. Leithoff,[26] T. Lenz,[26] C. Li,[59] Cheng Li,[55,43] D. M. Li,[63] F. Li,[1,43] F. Y. Li,[35] G. Li,[1] H. B. Li,[1,47] H. J. Li,[9,j] J. C. Li,[1] J. W. Li,[41] Ke Li,[1] L. K. Li,[1] Lei Li,[3] P. L. Li,[55,43] P. R. Li,[30] Q. Y. Li,[37] W. D. Li,[1,47] W. G. Li,[1] X. H. Li,[55,43] X. L. Li,[37] X. N. Li,[1,43] Z. B. Li,[44] Z. Y. Li,[44] H. Liang,[55,43] H. Liang,[1,47] Y. F. Liang,[40] Y. T. Liang,[28] G. R. Liao,[12] L. Z. Liao,[1,47] J. Libby,[21] C. X. Lin,[44] D. X. Lin,[15] Y. J. Lin,[13] B. Liu,[38,h] B. J. Liu,[1] C. X. Liu,[1] D. Liu,[55,43] D. Y. Liu,[38,h] F. H. Liu,[39] Fang Liu,[1] Feng Liu,[6] H. B. Liu,[13] H. M. Liu,[1,47] Huanhuan Liu,[1] Huihui Liu,[17] J. B. Liu,[55,43] J. Y. Liu,[1,47] K. Y. Liu,[31] Ke Liu,[6,*] L. Y. Liu,[13] Q. Liu,[47] S. B. Liu,[55,43] T. Liu,[1,47] X. Liu,[30] X. Y. Liu,[1,47] Y. B. Liu,[34] Z. A. Liu,[1,43,47] Zhiqing Liu,[37] Y. F. Long,[35] X. C. Lou,[1,43,47] H. J. Lu,[18] J. D. Lu,[1,47] J. G. Lu,[1,43] Y. Lu,[1] Y. P. Lu,[1,43] C. L. Luo,[32] M. X. Luo,[62] P. W. Luo,[44] T. Luo,[9,j] X. L. Luo,[1,43] S. Lusso,[58c] X. R. Lyu,[47] F. C. Ma,[31] H. L. Ma,[1] L. L. Ma,[37] M. M. Ma,[1,47] Q. M. Ma,[1] X. N. Ma,[34] X. X. Ma,[1,47] X. Y. Ma,[1,43] Y. M. Ma,[37] F. E. Maas,[15] M. Maggiora,[58a,58c] S. Maldaner,[26] S. Malde,[53] Q. A. Malik,[57] A. Mangoni,[23b] Y. J. Mao,[35] Z. P. Mao,[1] S. Marcello,[58a,58c] Z. X. Meng,[49] J. G. Messchendorp,[29] G. Mezzadri,[24a] J. Min,[1,43] T. J. Min,[33] R. E. Mitchell,[22] X. H. Mo,[1,43,47] Y. J. Mo,[6] C. Morales Morales,[15] N. Yu. Muchnoi,[10,d] H. Muramatsu,[51] A. Mustafa,[4] S. Nakhoul,[11,g] Y. Nefedov,[27] F. Nerling,[11,g] I. B. Nikolaev,[10,d] Z. Ning,[1,43] S. Nisar,[8,k] S. L. Niu,[1,43] S. L. Olsen,[47] Q. Ouyang,[1,43,47] S. Pacetti,[23b] Y. Pan,[55,43] M. Papenbrock,[59] P. Patteri,[23a] M. Pelizaeus,[4] H. P. Peng,[55,43] K. Peters,[11,g] J. Pettersson,[59] J. L. Ping,[32] R. G. Ping,[1,47] A. Pitka,[4] R. Poling,[51] V. Prasad,[55,43] H. R. Qi,[2] M. Qi,[33] T. Y. Qi,[2] S. Qian,[1,43] C. F. Qiao,[47] N. Qin,[60] X. P. Qin,[13] X. S. Qin,[4] Z. H. Qin,[1,43] J. F. Qiu,[1] S. Q. Qu,[34] K. H. Rashid,[57,i] K. Ravindran,[21] C. F. Redmer,[26] M. Richter,[4] A. Rivetti,[58c] V. Rodin,[29] M. Rolo,[58c] G. Rong,[1,47] Ch. Rosner,[15] M. Rump,[52] A. Sarantsev,[27,e] M. Savrié,[24b] Y. Schelhaas,[26] K. Schoenning,[59] W. Shan,[19] X. Y. Shan,[55,43] M. Shao,[55,43] C. P. Shen,[2] P. X. Shen,[34] X. Y. Shen,[1,47] H. Y. Sheng,[1] X. Shi,[1,43] X. D. Shi,[55,43] J. J. Song,[37] Q. Q. Song,[55,43] X. Y. Song,[1] S. Sosio,[58a,58c] C. Sowa,[4] S. Spataro,[58a,58c] F. F. Sui,[37] G. X. Sun,[1] J. F. Sun,[16] L. Sun,[60] S. S. Sun,[1,47] X. H. Sun,[1] Y. J. Sun,[55,43] Y. K. Sun,[55,43] Y. Z. Sun,[1] Z. J. Sun,[1,43] Z. T. Sun,[1] Y. T. Tan,[55,43] C. J. Tang,[40] G. Y. Tang,[1] X. Tang,[1] V. Thoren,[59] B. Tsednee,[25] I. Uman,[46d] B. Wang,[1] B. L. Wang,[47] C. W. Wang,[33] D. Y. Wang,[35] K. Wang,[1,43] L. L. Wang,[1] L. S. Wang,[1] M. Wang,[37] M. Z. Wang,[35] Meng Wang,[1,47] P. L. Wang,[1] R. M. Wang,[61] W. P. Wang,[55,43] X. Wang,[35] X. F. Wang,[1] X. L. Wang,[9,j] Y. Wang,[55,43] Y. Wang,[44] Y. F. Wang,[1,43,47] Z. Wang,[1,43] Z. G. Wang,[1,43] Z. Y. Wang,[1] Zongyuan Wang,[1,47] T. Weber,[4] D. H. Wei,[12] P. Weidenkaff,[26] H. W. Wen,[32] S. P. Wen,[1] U. Wiedner,[4] G. Wilkinson,[53] M. Wolke,[59] L. H. Wu,[1] L. J. Wu,[1,47] Z. Wu,[1,43] L. Xia,[55,43] Y. Xia,[20] S. Y. Xiao,[1] Y. J. Xiao,[1,47] Z. J. Xiao,[32] Y. G. Xie,[1,43] Y. H. Xie,[6] T. Y. Xing,[1,47] X. A. Xiong,[1,47] Q. L. Xiu,[1,43] G. F. Xu,[1] J. J. Xu,[33] L. Xu,[1] Q. J. Xu,[14] W. Xu,[1,47] X. P. Xu,[41] F. Yan,[56] L. Yan,[58a,58c] W. B. Yan,[55,43] W. C. Yan,[2] Y. H. Yan,[20] H. J. Yang,[38,h] H. X. Yang,[1] L. Yang,[60] R. X. Yang,[55,43] S. L. Yang,[1,47] Y. H. Yang,[33] Y. X. Yang,[12] Yifan Yang,[1,47] Z. Q. Yang,[20] M. Ye,[1,43] M. H. Ye,[7] J. H. Yin,[1] Z. Y. You,[44] B. X. Yu,[1,43,47] C. X. Yu,[34] J. S. Yu,[20] T. Yu,[56] C. Z. Yuan,[1,47] X. Q. Yuan,[35] Y. Yuan,[1] A. Yuncu,[46b,a] A. A. Zafar,[57] Y. Zeng,[20] B. X. Zhang,[1] B. Y. Zhang,[1,43] C. C. Zhang,[1] D. H. Zhang,[1] H. H. Zhang,[44]

H. Y. Zhang,[1,43] J. Zhang,[1,47] J. L. Zhang,[61] J. Q. Zhang,[4] J. W. Zhang,[1,43,47] J. Y. Zhang,[1] J. Z. Zhang,[1,47] K. Zhang,[1,47] L. Zhang,[45] S. F. Zhang,[33] T. J. Zhang,[38,h] X. Y. Zhang,[37] Y. Zhang,[55,43] Y. H. Zhang,[1,43] Y. T. Zhang,[55,43] Yang Zhang,[1] Yao Zhang,[1] Yi Zhang,[9,j] Yu Zhang,[47] Z. H. Zhang,[6] Z. P. Zhang,[55] Z. Y. Zhang,[60] G. Zhao,[1] J. W. Zhao,[1,43] J. Y. Zhao,[1,47] J. Z. Zhao,[1,43] Lei Zhao,[55,43] Ling Zhao,[1] M. G. Zhao,[34] Q. Zhao,[1] S. J. Zhao,[63] T. C. Zhao,[1] Y. B. Zhao,[1,43] Z. G. Zhao,[55,43] A. Zhemchugov,[27,b] B. Zheng,[56] J. P. Zheng,[1,43] Y. Zheng,[35] Y. H. Zheng,[47] B. Zhong,[32] L. Zhou,[1,43] L. P. Zhou,[1,47] Q. Zhou,[1,47] X. Zhou,[60] X. K. Zhou,[47] X. R. Zhou,[55,43] Xiaoyu Zhou,[20] Xu Zhou,[20] A. N. Zhu,[1,47] J. Zhu,[34] J. Zhu,[44] K. Zhu,[1] K. J. Zhu,[1,43,47] S. H. Zhu,[54] W. J. Zhu,[34] X. L. Zhu,[45] Y. C. Zhu,[55,43] Y. S. Zhu,[1,47] Z. A. Zhu,[1,47] J. Zhuang,[1,43] B. S. Zou,[1] and J. H. Zou[1]

(BESIII Collaboration)

[1]*Institute of High Energy Physics, Beijing 100049, People's Republic of China*
[2]*Beihang University, Beijing 100191, People's Republic of China*
[3]*Beijing Institute of Petrochemical Technology, Beijing 102617, People's Republic of China*
[4]*Bochum Ruhr-University, D-44780 Bochum, Germany*
[5]*Carnegie Mellon University, Pittsburgh, Pennsylvania 15213, USA*
[6]*Central China Normal University, Wuhan 430079, People's Republic of China*
[7]*China Center of Advanced Science and Technology, Beijing 100190, People's Republic of China*
[8]*COMSATS University Islamabad, Lahore Campus, Defence Road, Off Raiwind Road, 54000 Lahore, Pakistan*
[9]*Fudan University, Shanghai 200443, People's Republic of China*
[10]*G.I. Budker Institute of Nuclear Physics SB RAS (BINP), Novosibirsk 630090, Russia*
[11]*GSI Helmholtzcentre for Heavy Ion Research GmbH, D-64291 Darmstadt, Germany*
[12]*Guangxi Normal University, Guilin 541004, People's Republic of China*
[13]*Guangxi University, Nanning 530004, People's Republic of China*
[14]*Hangzhou Normal University, Hangzhou 310036, People's Republic of China*
[15]*Helmholtz Institute Mainz, Johann-Joachim-Becher-Weg 45, D-55099 Mainz, Germany*
[16]*Henan Normal University, Xinxiang 453007, People's Republic of China*
[17]*Henan University of Science and Technology, Luoyang 471003, People's Republic of China*
[18]*Huangshan College, Huangshan 245000, People's Republic of China*
[19]*Hunan Normal University, Changsha 410081, People's Republic of China*
[20]*Hunan University, Changsha 410082, People's Republic of China*
[21]*Indian Institute of Technology Madras, Chennai 600036, India*
[22]*Indiana University, Bloomington, Indiana 47405, USA*
[23a]*INFN Laboratori Nazionali di Frascati, I-00044 Frascati, Italy*
[23b]*INFN and University of Perugia, I-06100 Perugia, Italy*
[24a]*INFN Sezione di Ferrara, I-44122 Ferrara, Italy*
[24b]*University of Ferrara, I-44122 Ferrara, Italy*
[25]*Institute of Physics and Technology, Peace Avenue 54B, Ulaanbaatar 13330, Mongolia*
[26]*Johannes Gutenberg University of Mainz, Johann-Joachim-Becher-Weg 45, D-55099 Mainz, Germany*
[27]*Joint Institute for Nuclear Research, 141980 Dubna, Moscow region, Russia*
[28]*Justus-Liebig-Universitaet Giessen, II. Physikalisches Institut, Heinrich-Buff-Ring 16, D-35392 Giessen, Germany*
[29]*KVI-CART, University of Groningen, NL-9747 AA Groningen, Netherlands*
[30]*Lanzhou University, Lanzhou 730000, People's Republic of China*
[31]*Liaoning University, Shenyang 110036, People's Republic of China*
[32]*Nanjing Normal University, Nanjing 210023, People's Republic of China*
[33]*Nanjing University, Nanjing 210093, People's Republic of China*
[34]*Nankai University, Tianjin 300071, People's Republic of China*
[35]*Peking University, Beijing 100871, People's Republic of China*
[36]*Shandong Normal University, Jinan 250014, People's Republic of China*
[37]*Shandong University, Jinan 250100, People's Republic of China*
[38]*Shanghai Jiao Tong University, Shanghai 200240, People's Republic of China*
[39]*Shanxi University, Taiyuan 030006, People's Republic of China*
[40]*Sichuan University, Chengdu 610064, People's Republic of China*
[41]*Soochow University, Suzhou 215006, People's Republic of China*
[42]*Southeast University, Nanjing 211100, People's Republic of China*
[43]*State Key Laboratory of Particle Detection and Electronics, Beijing 100049, Hefei 230026, People's Republic of China*
[44]*Sun Yat-Sen University, Guangzhou 510275, People's Republic of China*
[45]*Tsinghua University, Beijing 100084, People's Republic of China*

[46a]Ankara University, 06100 Tandogan, Ankara, Turkey
[46b]Istanbul Bilgi University, 34060 Eyup, Istanbul, Turkey
[46c]Uludag University, 16059 Bursa, Turkey
[46d]Near East University, Nicosia, North Cyprus, Mersin 10, Turkey
[47]University of Chinese Academy of Sciences, Beijing 100049, People's Republic of China
[48]University of Hawaii, Honolulu, Hawaii 96822, USA
[49]University of Jinan, Jinan 250022, People's Republic of China
[50]University of Manchester, Oxford Road, Manchester M13 9PL, United Kingdom
[51]University of Minnesota, Minneapolis, Minnesota 55455, USA
[52]University of Muenster, Wilhelm-Klemm-Str. 9, 48149 Muenster, Germany
[53]University of Oxford, Keble Rd, Oxford, United Kingdom OX13RH
[54]University of Science and Technology Liaoning, Anshan 114051, People's Republic of China
[55]University of Science and Technology of China, Hefei 230026, People's Republic of China
[56]University of South China, Hengyang 421001, People's Republic of China
[57]University of the Punjab, Lahore-54590, Pakistan
[58a]University of Turin, I-10125 Turin, Italy
[58b]University of Eastern Piedmont, I-15121 Alessandria, Italy
[58c]INFN, I-10125 Turin, Italy
[59]Uppsala University, Box 516, SE-75120 Uppsala, Sweden
[60]Wuhan University, Wuhan 430072, People's Republic of China
[61]Xinyang Normal University, Xinyang 464000, People's Republic of China
[62]Zhejiang University, Hangzhou 310027, People's Republic of China
[63]Zhengzhou University, Zhengzhou 450001, People's Republic of China

(Received 25 July 2019; revised manuscript received 1 October 2019; published 2 December 2019)

By analyzing a 2.93 fb^{-1} data sample of e^+e^- collisions, recorded at a center-of-mass energy of 3.773 GeV with the BESIII detector operated at the BEPCII collider, we report the first observation of the semileptonic D^+ transition into the axial-vector meson $D^+ \to \bar{K}_1(1270)^0 e^+\nu_e$ with a statistical significance greater than 10σ. Its decay branching fraction is determined to be $\mathcal{B}[D^+ \to \bar{K}_1(1270)^0 e^+\nu_e] = (2.30 \pm 0.26^{+0.18}_{-0.21} \pm 0.25) \times 10^{-3}$, where the first and second uncertainties are statistical and systematic, respectively, and the third originates from the input branching fraction of $\bar{K}_1(1270)^0 \to K^-\pi^+\pi^0$.

DOI: 10.1103/PhysRevLett.123.231801

Studies of semileptonic (SL) D transitions, mediated via $c \to s(d)\ell^+\nu_\ell$ at the quark level, are important for the understanding of nonperturbative strong-interaction dynamics in weak decays [1,2]. Those transitions into S-wave states have been extensively studied in theory and experiment. However, there is still no experimental confirmation of the predicted transitions into P-wave states.

In the quark model, the physical mass eigenstates of the strange axial-vector mesons, $K_1(1270)$ and $K_1(1400)$, are mixtures of the $^1P_1$ and $^3P_1$ states with a mixing angle θ_{K_1}. These mesons have been thoroughly studied via τ, B, D, $\psi(3686)$, and J/ψ decays, as well as via Kp scattering [3–12]. Nevertheless, the value of θ_{K_1} is still very controversial in various phenomenological analyses [13–20]. Studies of the SL D transitions into $\bar{K}_1(1270)$ provide important insight into the mixing angle θ_{K_1}. The improved knowledge of θ_{K_1} is essential for theoretical calculations describing the decays of τ [13], B [15,21], and D [22,23] particles into strange axial-vector mesons, and for investigations in the field of hadron spectroscopy [24].

Earlier quantitative predictions for the branching fractions (BFs) of $D^{0(+)} \to \bar{K}_1(1270)e^+\nu_e$ were derived from the Isgur-Scora-Grinstein-Wise (ISGW) quark model [1] and its update, ISGW2 [2]. ISGW2 implies that the BFs of $D^{0(+)} \to \bar{K}_1(1270)e^+\nu_e$ are about 0.1 (0.3)%. However, the model ignores the mixing between $^1P_1$ and $^3P_1$ states. Recently, the rates of these decays were calculated with three-point QCD sum rules (3PSRs) [25], the covariant light-front quark model (CLFQM) [26], and light-cone QCD sum rules (LCSRs) [27]. In general, the predicted BFs range from 10^{-3} to 10^{-2} [25–27], and are sensitive to θ_{K_1} and its sign. Measurements of $D^{0(+)} \to \bar{K}_1(1270)e^+\nu_e$ will be critical to distinguish between theoretical calculations, to explore the nature of strange axial-vector mesons, and to understand the weak-decay mechanisms of D mesons.

Currently, there is very little experimental information available about semileptonic D decays into axial-vector

mesons, with the only result being the reported evidence for the process $D^0 \to K_1(1270)^- e^+ \nu_e$ from the CLEO Collaboration [28]. This Letter presents the first observation of $D^+ \to \bar{K}_1(1270)^0 e^+ \nu_e$ [29] by using an e^+e^- data sample corresponding to an integrated luminosity of 2.93 fb^{-1} [30] recorded at a center-of-mass energy of $\sqrt{s} = 3.773$ GeV with the BESIII detector [31].

Details about the design and performance of the BESIII detector are given in Ref. [31]. Simulated samples produced with the GEANT4-based [32] Monte Carlo (MC) package, which includes the geometric description of the BESIII detector and the detector response, are used to determine the detection efficiency and to estimate the backgrounds. The simulation includes the beam-energy spread and initial-state radiation (ISR) in the e^+e^- annihilations modeled with the generator KKMC [33]. The inclusive MC samples consist of the production of the $D\bar{D}$ pairs, the non-$D\bar{D}$ decays of the $\psi(3770)$, the ISR production of the J/ψ and $\psi(3686)$ states, and the continuum processes incorporated in KKMC [33]. The known decay modes are modeled with EVTGEN [34] using BFs taken from the Particle Data Group [35], and the remaining unknown decays from the charmonium states with LUNDCHARM [36]. The final-state radiation (FSR) from charged final-state particles are incorporated with the PHOTOS package [37]. The $D^+ \to \bar{K}_1(1270)^0 e^+ \nu_e$ decay is simulated with the ISGW2 model [38], the $\bar{K}_1(1270)^0$ is set to decay into all possible processes containing the $K^-\pi^+\pi^0$ combination. The resonance shape of $\bar{K}_1(1270)^0$ is parametrized by a relativistic Breit-Wigner function, and the mass and width of $\bar{K}_1(1270)^0$ are fixed at the world-average values 1272 ± 7 MeV and 90 ± 20 MeV, respectively [35].

The measurement employs the $e^+e^- \to \psi(3770) \to D^+D^-$ decay chain. The D^- mesons are reconstructed by their hadronic decays to $K^+\pi^-\pi^-$, $K^0_S\pi^-$, $K^+\pi^-\pi^-\pi^0$, $K^0_S\pi^-\pi^0$, $K^0_S\pi^+\pi^-\pi^-$, and $K^+K^-\pi^-$. These inclusively selected events are referred to as single-tag (ST) D^- mesons. In the presence of the ST D^- mesons, candidate $D^+ \to \bar{K}_1(1270)^0 e^+ \nu_e$ decays are selected to form double-tag (DT) events. The BF of $D^+ \to \bar{K}_1(1270)^0 e^+ \nu_e$ is given by

$$\mathcal{B}_{\rm SL} = N_{\rm DT}/(N^{\rm tot}_{\rm ST}\varepsilon_{\rm SL}), \quad (1)$$

where $N^{\rm tot}_{\rm ST}$ and $N_{\rm DT}$ are the ST and DT yields in the data sample, $\varepsilon_{\rm SL} = \Sigma_i[(\varepsilon^i_{\rm DT}N^i_{\rm ST})/(\varepsilon^i_{\rm ST}N^{\rm tot}_{\rm ST})]$ is the efficiency of detecting the SL decay in the presence of the ST D^- meson. Here i denotes the tag mode, and $\varepsilon_{\rm ST}$ and $\varepsilon_{\rm DT}$ are the ST and DT efficiencies of selecting the ST and DT candidates, respectively.

We use the same selection criteria as discussed in Refs. [39–41]. All charged tracks are required to be within a polar-angle (θ) range of $|\cos\theta| < 0.93$. All of them, except for those from K^0_S decays, must originate from an interaction region defined by $V_{xy} < 1$ cm and $|V_z| < 10$ cm. Here, V_{xy} and $|V_z|$ denote the distances of closest approach of the reconstructed track to the interaction point (IP) in the xy plane and the z direction (along the beam), respectively.

Particle identification (PID) of charged kaons and pions is performed using the specific ionization energy loss (dE/dx) measured by the main drift chamber (MDC) and the time of flight. Positron PID also uses the measured information from the electromagnetic calorimeter (EMC). The combined confidence levels under the positron, pion, and kaon hypotheses (CL_e, CL_π and CL_K, respectively) are calculated. Kaon (pion) candidates are required to satisfy $CL_K > CL_\pi$ ($CL_\pi > CL_K$). Positron candidates are required to satisfy $CL_e > 0.001$ and $CL_e/(CL_e + CL_\pi + CL_K) > 0.8$. To reduce the background from hadrons and muons, the positron candidate is further required to have a deposited energy in the EMC greater than 0.8 times its momentum in the MDC.

K^0_S candidates are reconstructed from two oppositely charged tracks satisfying $|V_z| < 20$ cm. The two charged tracks are assigned as $\pi^+\pi^-$ without imposing further PID criteria. They are constrained to originate from a common vertex and are required to have an invariant mass within $|M_{\pi^+\pi^-} - M_{K^0_S}| < 12$ MeV/c^2, where $M_{K^0_S}$ is the K^0_S nominal mass [35]. The decay length of the K^0_S candidate is required to be greater than twice the vertex resolution away from the IP.

Photon candidates are selected using the information from the EMC. It is required that the shower time is within 700 ns of the event start time, the shower energy be greater than 25 (50) MeV if the crystal with the maximum deposited energy in that cluster is in the barrel (end-cap) region [31], and the opening angle between the candidate shower and any charged tracks is greater than 10°. Neutral π^0 candidates are selected from the photon pairs with the invariant mass within $(0.115, 0.150)$ GeV/c^2. The momentum resolution of the accepted photon pair is improved by a kinematic fit, which constrains the $\gamma\gamma$ invariant mass to the π^0 nominal mass [35].

The ST D^- mesons are distinguished from the combinatorial backgrounds by two variables: the energy difference $\Delta E = E_{D^-} - E_{\rm beam}$ and the beam-energy constrained mass $M_{\rm BC} = \sqrt{E^2_{\rm beam} - |\vec{p}_{D^-}|^2}$, where $E_{\rm beam}$ is the beam energy, and $\vec{p}_{D^-}$ and E_{D^-} are the measured momentum and energy of the ST candidate in the e^+e^- center-of-mass frame, respectively. For each tag mode, only the one with the minimum $|\Delta E|$ is kept. The combinatorial backgrounds in the $M_{\rm BC}$ distributions are suppressed by requiring ΔE within $(-55, +40)$ MeV for the tag modes involving a π^0, and $(-25, +25)$ MeV for the other tag modes.

Figure 1 shows the $M_{\rm BC}$ distributions of the accepted ST candidates in the data sample for various tag modes. The ST yield for each tag mode is obtained by performing a

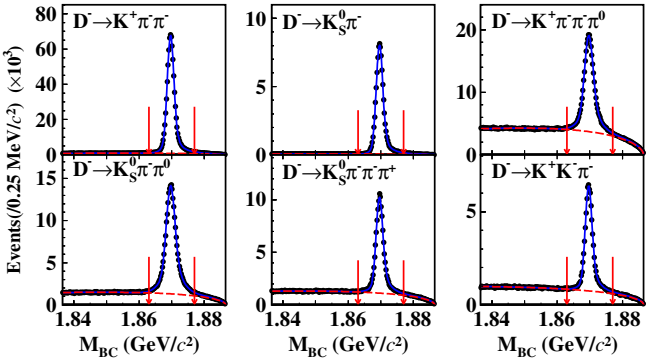

FIG. 1. The $M_{\rm BC}$ distributions of the ST candidates in the data sample (dots with error bars). Blue solid curves are the fit results and red dashed curves represent the background contributions of the fit. The pair of red arrows in each subfigure indicate the $M_{\rm BC}$ window.

maximum-likelihood fit to the corresponding $M_{\rm BC}$ distribution. In the fits, the D^- signal is modeled by a MC-simulated $M_{\rm BC}$ shape convolved with a double-Gaussian function and the combinatorial-background shape is described by an ARGUS function [42]. The candidates in the $M_{\rm BC}$ signal region, $(1.863, 1.877)$ GeV/c^2, are kept for further analysis. The total ST yield is $N^{\rm tot}_{\rm ST} = 1522474 \pm 2215$, where the uncertainty is statistical.

In the analysis of the particles recoiling against the ST D^- mesons, candidate events for the $D^+ \to \bar{K}_1(1270)^0 e^+ \nu_e$ channel are selected from the remaining tracks that have not been used for the ST reconstruction. The $\bar{K}_1(1270)^0$ meson is reconstructed using its dominant decay $\bar{K}_1(1270)^0 \to K^- \pi^+ \pi^0$. It is required that there are only three good charged tracks available for this selection. One of the tracks with charge opposite to that of the D^- tag is identified as the positron. The other two oppositely charged tracks are identified as a kaon and a pion, according to their PID information. Moreover, the kaon candidate must have charge opposite to that of the positron. Other selection criteria, which have been optimized by analyzing the inclusive MC samples, are as follows.

To effectively veto the backgrounds associated with wrongly paired photons, the π^0 candidates must have a momentum greater than 0.15 GeV/c and a decay angle $|\cos\theta_{{\rm decay},\pi^0}| = |E_{\gamma_1} - E_{\gamma_2}|/|\vec{p}_{\pi^0}|$ less than 0.8. Here, E_{γ_1} and E_{γ_2} are the energies of γ_1 and γ_2, and $\vec{p}_{\pi^0}$ is the momentum of the π^0 candidate. To suppress the potential backgrounds from the hadronic decays $D^+ \to K^- \pi^+ \pi^+ \pi^0$, the invariant mass of the $K^- \pi^+ \pi^0 e^+$ combination, $M_{K^-\pi^+\pi^0 e^+}$, is required to be smaller than 1.78 GeV/c^2.

Information concerning the undetectable neutrino is inferred by the kinematic quantity $U_{\rm miss} \equiv E_{\rm miss} - |\vec{p}_{\rm miss}|$, where $E_{\rm miss}$ and $\vec{p}_{\rm miss}$ are the missing energy and momentum of the SL candidate, respectively, calculated by $E_{\rm miss} \equiv E_{\rm beam} - \Sigma_j E_j$ and $\vec{p}_{\rm miss} \equiv \vec{p}_{D^+} - \Sigma_j \vec{p}_j$ in the e^+e^- center-of-mass frame. The index j sums over the K^-, π^+, π^0, and e^+ of the signal candidate, and E_j and $\vec{p}_j$ are the energy and momentum of the jth particle, respectively. To improve the $U_{\rm miss}$ resolution, the D^+ energy is constrained to the beam energy and $\vec{p}_{D^+} \equiv -\hat{p}_{D^-}\sqrt{E^2_{\rm beam} - m^2_{D^+}}$, where $\hat{p}_{D^-}$ is the unit vector in the momentum direction of the ST D^-, and m_{D^+} is the D^+ nominal mass [35]. To partially recover the effects of FSR and bremsstrahlung (FSR recovery), the four-momenta of photon(s) within 5° of the initial positron direction are added to the positron four-momentum measured by the MDC.

Events that originate from the process $D^+ \to \bar{K}^*(892)^0[\to K^-\pi^+]e^+\nu_e$, in which a fake π^0 is wrongly associated to the signal decay, form a peaking background around +0.02 GeV in the $U_{\rm miss}$ distribution and around 1.15 GeV/c^2 in the $M_{K^-\pi^+\pi^0}$ distribution. To suppress these backgrounds, we define an alternative kinematic quantity $U'_{\rm miss} \equiv E'_{\rm miss} - |\vec{p}'_{\rm miss}|$, where $E'_{\rm miss} \equiv E_{\rm beam} - \Sigma_j E_j$ and $\vec{p}'_{\rm miss} \equiv \vec{p}_{D^+} - \Sigma_j \vec{p}_j$, and j only sums over the K^-, π^+, and e^+ candidates of the signal candidate. Since these backgrounds form an obvious peak around zero in the $U'_{\rm miss}$ distribution, the $U'_{\rm miss}$ values of the SL candidates are required to lie outside $(-0.09, 0.03)$ GeV.

Figure 2(a) shows the distribution of $M_{K^-\pi^+\pi^0}$ vs $U_{\rm miss}$ of the accepted $D^+ \to K^-\pi^+\pi^0 e^+\nu_e$ candidate events in the

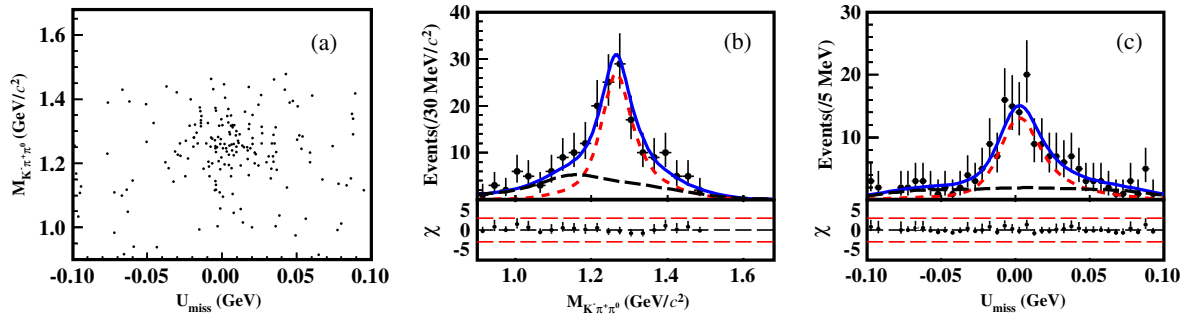

FIG. 2. (a) The $M_{K^-\pi^+\pi^0}$ vs $U_{\rm miss}$ distribution of the SL candidate events and (b), (c) the projections to $M_{K^-\pi^+\pi^0}$ and $U_{\rm miss}$, respectively, with the residual χ distributions of the 2D fit. Dots with error bars are data. Blue solid, red, and black dashed curves are the fit result, the fitted signal, and the fitted background, respectively.

data sample after combining all tag modes. A clear signal, which concentrates around 1.27 GeV/c^2 in the $M_{K^-\pi^+\pi^0}$ distribution and around zero in the $U_{\rm miss}$ distribution, can be seen. The DT yield is obtained from a two-dimensional (2D) unbinned extended maximum-likelihood fit of the data presented by the distribution in Fig. 2(a). In the fit, the 2D signal shape is described by the MC-simulated shape extracted from the signal MC events of $D^+ \to \bar{K}_1(1270)^0 e^+\nu_e$. The 2D background shape is modeled by the MC-simulated shape obtained from the inclusive MC samples and the number of background events is a free parameter in the fit. The smooth 2D probability density functions of signal and background are modeled by the corresponding MC-simulated shape [43,44]. The projections of the 2D fit on the $M_{K^-\pi^+\pi^0}$ and $U_{\rm miss}$ distributions are shown in Figs. 2(b) and 2(c). In the fit, we ignore the contributions from nonresonant decays $D^+ \to K^-\pi^+\pi^0 e^+\nu_e$, $\bar{K}^*(892)^0\pi^0 e^+\nu_e$, $K^*(892)^-\pi^+ e^+\nu_e$, and $K^-\rho(770)^+ e^+\nu_e$, as well as the possible interference between them due to the low significance of these contributions with the limited size of the data set. The two decays $D^+ \to \bar{K}_1(1400)^0 e^+\nu_e$ and $D^+ \to \bar{K}^*(1430)^0 e^+\nu_e$ are indistinguishable, and as no significant contribution is found from either source, these components are not included in the fit. From the fit, we obtain the DT yield of $N_{\rm DT} = 119.7 \pm 13.3$, where the uncertainty is statistical. The statistical significance of the signal is estimated to be greater than 10σ, by comparing the likelihoods with and without the signal components included, and taking the change in the number of degrees of freedom into account.

For each tag mode, the DT efficiency is estimated with the corresponding signal MC events. The average signal efficiency is determined to be $\varepsilon_{\rm SL} = 0.0742 \pm 0.0007$. Compared to $\epsilon_{\rm SL}$, the signal efficiencies for individual tag modes vary within $\pm 10\%$. The reliability of the MC simulation is tested by examining typical distributions of the SL candidate events. The data distributions of momenta and $\cos\theta$ of K^-, π^+, π^0, and e^+ are consistent with those of MC simulations.

By inserting $N_{\rm DT}$, $\varepsilon_{\rm SL}$, and $N_{\rm ST}^{\rm tot}$ into Eq. (1), we determine the product of $\mathcal{B}_{\rm SL}$ and the BF of $\bar{K}_1(1270)^0 \to K^-\pi^+\pi^0$ ($\mathcal{B}_{\rm sub}$) to be

$$\mathcal{B}_{\rm SL}\mathcal{B}_{\rm sub} = (1.06 \pm 0.12^{+0.08}_{-0.10}) \times 10^{-3},$$

where the first and second uncertainties are statistical and systematic, respectively.

The systematic uncertainties in the BF measurement, which are assigned relative to the measured BF, are discussed below. The DT method ensures that most uncertainties arising from the ST selection cancel. The uncertainty from the ST yield is assigned to be 0.5% [39–41], by examining the relative change in the yield between data and MC simulation after varying the $M_{\rm BC}$ fit range, the signal shape, and the endpoint of the ARGUS function.

The uncertainties associated with the efficiencies of e^+ tracking (PID), K^- tracking (PID), π^+ tracking (PID), and π^0 reconstruction are investigated using data and MC samples of $e^+e^- \to \gamma e^+e^-$ events and DT $D\bar{D}$ hadronic events. Small differences between the data and MC efficiencies are found, which are $-(0.03 \pm 0.15)\%$, $+(0.94 \pm 0.27)\%$, $+(2.63 \pm 0.32)\%$, $-(0.14 \pm 0.18)\%$, $+(0.03 \pm 0.13)\%$, $-(0.08 \pm 0.18)\%$ for e^+ tracking, e^+ PID, K^- tracking, K^- PID, π^+ tracking, and π^+ PID, respectively. The MC efficiency is then corrected by these differences and used to determine the central value of the BF. In the studies of e^+ tracking (PID) efficiencies, the 2D (momentum and $\cos\theta$) tracking efficiencies of data and MC simulation of $e^+e^- \to \gamma e^+e^-$ events are reweighted to match those of $D^+ \to \bar{K}_1(1270)^0 e^+\nu_e$ decays. After corrections, we assign the uncertainties associated with the e^+ tracking (PID), K^- tracking (PID), π^+ tracking (PID), and π^0 reconstruction to be 1.0% (1.0%), 1.0% (0.5%), 0.5% (0.5%), and 2.0%, respectively.

The uncertainty associated with the $M_{K^-\pi^+\pi^0 e^+}$ requirement is estimated by varying the requirement by ± 0.05 GeV/c^2, and the largest change on the BF, 0.9%, is taken as the systematic uncertainty. Similarly, the systematic uncertainty in the $U'_{\rm miss}$ requirement is estimated to be 1.7% by varying the corresponding selection window by ± 0.01 GeV. The uncertainty of the input BFs of $\bar{K}_1(1270)^0$ is estimated by changing the BF of each subdecay by $\pm 1\sigma$. The largest variation in the detection efficiency, 0.5%, is assigned as the related systematic uncertainty. The uncertainty of the 2D fit is estimated to be $^{+7.0\%}_{-8.2\%}$ by examining the BF changes with different fit ranges, signal shapes (dominated by varying the width of $\bar{K}_1(1270)^0$ by $\pm 1\sigma$), and background shapes. The uncertainty arising from background shapes is mainly due to unknown nonresonant decays, and is assigned as the change of the fitted DT yield when they are fixed by referring to the well-known nonresonant fraction in $D^+ \to \bar{K}^*(892)^0 e^+\nu_e$ [45]. The uncertainty arising from the limited size of the MC samples is 1.0%.

The uncertainty due to FSR recovery is evaluated to be 1.3% which is the change of the BF when varying the FSR recovery angle to be 10°. The total systematic uncertainty is estimated to be $^{+8.0\%}_{-9.0\%}$ by adding all the individual contributions in quadrature.

When making use of the world average of $\mathcal{B}_{\rm sub} = 0.467 \pm 0.050$ [35,46], we obtain

$$\mathcal{B}_{\rm SL} = (2.30 \pm 0.26^{+0.18}_{-0.21} \pm 0.25) \times 10^{-3},$$

where the third uncertainty, 10.7%, is from the external uncertainty of the input BF $\mathcal{B}_{\rm sub}$.

To summarize, by analyzing an e^+e^- collision data sample of 2.93 fb^{-1} taken at $\sqrt{s} = 3.773$ GeV, we report the observation of $D^+ \to \bar{K}_1(1270)^0 e^+\nu_e$ and determine its

decay BF for the first time. The measured BF is 1.4% of the total semileptonic D^+ decay width, which lies between the ISGW prediction of 1% and the ISGW2 prediction of 2%. Our BF of $D^+ \to \bar{K}_1(1270)^0 e^+ \nu_e$ agrees with the CLFQM and LCSR predictions when $\theta_{K_1} \approx 33°$ or 57° [26], and clearly rules out the predictions when setting θ_{K_1} negative [27]. Making use of the measured value for the BF of $D^0 \to K_1(1270)^- e^+ \nu_e$ [28] and the world-average lifetimes of the D^0 and D^+ mesons [35], we determine the partial decay width ratio $\Gamma[D^+ \to \bar{K}_1(1270)^0 e^+ \nu_e]/\Gamma[D^0 \to K_1(1270)^- e^+ \nu_e] = 1.2^{+0.7}_{-0.5}$, which is consistent with unity as predicted by isospin conservation. This demonstration of the capability to observe $\bar{K}_1(1270)$ mesons in the very clean environment of SL $D^{0(+)}$ decays opens up the opportunity to conduct further studies of the nature of these axial-vector mesons. A near-future follow-up analysis of the dynamics of these SL decays with higher statistics will allow for deeper explorations of the inner structure, production, mass and width of $\bar{K}_1(1270)$ and $\bar{K}_1(1400)$, as well as providing access to hadronic-transition form factors.

The BESIII collaboration thanks the staff of BEPCII and the IHEP computing center for their strong support. Authors thank helpful discussions from Xianwei Kang and Haiyang Cheng. This work is supported in part by National Key Basic Research Program of China under Contract No. 2015CB856700; National Natural Science Foundation of China (NSFC) under Contract No. 11835012; National Natural Science Foundation of China (NSFC) under Contracts No. 11775230, No. 11625523, No. 11635010, No. 11735014; the Chinese Academy of Sciences (CAS) Large-Scale Scientific Facility Program; Joint Large-Scale Scientific Facility Funds of the NSFC and CAS under Contracts No. U1532257, No. U1532258, No. U1732263, No. U1832107, No. U1832207; CAS Key Research Program of Frontier Sciences under Contracts No. QYZDJ-SSW-SLH003, No. QYZDJ-SSW-SLH040; 100 Talents Program of CAS; INPAC and Shanghai Key Laboratory for Particle Physics and Cosmology; German Research Foundation DFG under Contract No. Collaborative Research Center 502 CRC 1044, FOR 2359; Istituto Nazionale di Fisica Nucleare, Italy; Koninklijke Nederlandse Akademie van Wetenschappen (KNAW) under Contract No. 530-4CDP03; Ministry of Development of Turkey under Contract No. DPT2006K-120470; National Science and Technology fund; The Knut and Alice Wallenberg Foundation (Sweden) under Contract No. 2016.0157; The Royal Society, UK under Contract No. DH160214; The Swedish Research Council; U.S. Department of Energy under Contracts No. DE-FG02-05ER41374, No. DE-SC-0010118, No. DE-SC-0012069; University of Groningen (RuG) and the Helmholtzzentrum fuer Schwerionenforschung GmbH (GSI), Darmstadt.

[*]Corresponding author.
liuke@ihep.ac.cn
[a]Also at Bogazici University, 34342 Istanbul, Turkey.
[b]Also at the Moscow Institute of Physics and Technology, Moscow 141700, Russia.
[c]Also at the Functional Electronics Laboratory, Tomsk State University, Tomsk 634050, Russia.
[d]Also at the Novosibirsk State University, Novosibirsk 630090, Russia.
[e]Also at the NRC "Kurchatov Institute," PNPI, 188300 Gatchina, Russia.
[f]Also at Istanbul Arel University, 34295 Istanbul, Turkey.
[g]Also at Goethe University Frankfurt, 60323 Frankfurt am Main, Germany.
[h]Also at Key Laboratory for Particle Physics, Astrophysics and Cosmology, Ministry of Education; Shanghai Key Laboratory for Particle Physics and Cosmology; Institute of Nuclear and Particle Physics, Shanghai 200240, People's Republic of China.
[i]Also at Government College Women University, Sialkot—51310, Punjab, Pakistan.
[j]Also at Key Laboratory of Nuclear Physics and Ion-beam Application (MOE) and Institute of Modern Physics, Fudan University, Shanghai 200443, People's Republic of China.
[k]Also at Harvard University, Department of Physics, Cambridge, Massachusetts 02138, USA.

[1] N. Isgur, D. Scora, B. Grinstein, and M. B. Wise, Phys. Rev. D **39**, 799 (1989).
[2] D. Scora and N. Isgur, Phys. Rev. D **52**, 2783 (1995).
[3] R. Barate *et al.* (ALEPH Collaboration), Eur. Phys. J. C **11**, 599 (1999).
[4] G. Abbiendi *et al.* (OPAL Collaboration), Eur. Phys. J. C **13**, 197 (2000).
[5] D. M. Asner *et al.* (CLEO Collaboration), Phys. Rev. D **62**, 072006 (2000).
[6] K. Abe *et al.* (Belle Collaboration), Phys. Rev. Lett. **87**, 161601 (2001).
[7] H. Yang *et al.* (Belle Collaboration), Phys. Rev. Lett. **94**, 111802 (2005).
[8] J. M. Link *et al.* (FOCUS Collaboration), Phys. Lett. B **610**, 225 (2005).
[9] J. Z. Bai *et al.* (BES Collaboration), Phys. Rev. Lett. **83**, 1918 (1999).
[10] M. Ablikim *et al.* (BES Collaboration), Phys. Rev. D **72**, 092002 (2005).
[11] C. Daum *et al.* (ACCMOR Collaboration), Nucl. Phys. **B187**, 1 (1981).
[12] D. Aston *et al.*, Nucl. Phys. **B292**, 693 (1987).
[13] M. Suzuki, Phys. Rev. D **47**, 1252 (1993).
[14] F. Divotgey, L. Olbrich, and F. Giacosa, Eur. Phys. J. A **49**, 135 (2013).
[15] H. Hatanaka and K. C. Yang, Phys. Rev. D **77**, 094023 (2008); **78**, 059902(E) (2008).
[16] H. Y. Cheng, Phys. Lett. B **707**, 116 (2012).
[17] H. G. Blundell, S. Godfrey, and B. Phelps, Phys. Rev. D **53**, 3712 (1996).
[18] A. Tayduganov, E. Kou, and A. Le Yaouanc, Phys. Rev. D **85**, 074011 (2012).
[19] H. J. Lipkin, Phys. Lett. **72B**, 249 (1977).

[20] L. Burakovsky and T. Goldman, Phys. Rev. D **56**, R1368 (1997).
[21] H. Y. Cheng and C. K. Chua, Phys. Rev. D **69**, 094007 (2004); **81**, 059901(E) (2010).
[22] H. Y. Cheng and C. W. Chiang, Phys. Rev. D **81**, 074031 (2010).
[23] H. Y. Cheng, Phys. Rev. D **67**, 094007 (2003).
[24] L. Burakovsky and T. Goldman, Phys. Rev. D **57**, 2879 (1998).
[25] R. Khosravi, K. Azizi, and N. Ghahramany, Phys. Rev. D **79**, 036004 (2009).
[26] H. Y. Cheng and X. W. Kang, Eur. Phys. J. C **77**, 587 (2017); **77**, 863(E) (2017), and private communication.
[27] S. Momeni and R. Khosravi, J. Phys. G **46**, 105006 (2019).
[28] M. Artuso *et al.* (CLEO Collaboration), Phys. Rev. Lett. **99**, 191801 (2007).
[29] Throughout the Letter, charged conjugated modes are implied unless stated explicitly.
[30] M. Ablikim *et al.* (BESIII Collaboration), Chin. Phys. C **37**, 123001 (2013); Phys. Lett. B **753**, 629 (2016).
[31] M. Ablikim *et al.* (BESIII Collaboration), Nucl. Instrum. Methods Phys. Res., Sect. A **614**, 345 (2010).
[32] S. Agostinelli *et al.* (GEANT4 Collaboration), Nucl. Instrum. Methods Phys. Res., Sect. A **506**, 250 (2003).
[33] S. Jadach, B. F. L. Ward, and Z. Was, Phys. Rev. D **63**, 113009 (2001); Comput. Phys. Commun. **130**, 260 (2000).
[34] D. J. Lange, Nucl. Instrum. Methods Phys. Res., Sect. A **462**, 152 (2001); R. G. Ping, Chin. Phys. C **32**, 599 (2008).
[35] M. Tanabashi *et al.* (Particle Data Group), Phys. Rev. D **98**, 030001 (2018) and 2019 update.
[36] J. C. Chen, G. S. Huang, X. R. Qi, D. H. Zhang, and Y. S. Zhu, Phys. Rev. D **62**, 034003 (2000); R. L. Yang, R. G. Ping, and H. Chen, Chin. Phys. Lett. **31**, 061301 (2014).
[37] E. Richter-Was, Phys. Lett. B **303**, 163 (1993).
[38] D. Becirevic and A. B. Kaidalov, Phys. Lett. B **478**, 417 (2000).
[39] M. Ablikim *et al.* (BESIII Collaboration), Eur. Phys. J. C **76**, 369 (2016).
[40] M. Ablikim *et al.* (BESIII Collaboration), Chin. Phys. C **40**, 113001 (2016).
[41] M. Ablikim *et al.* (BESIII Collaboration), Phys. Rev. Lett. **121**, 171803 (2018).
[42] H. Albrecht *et al.* (ARGUS Collaboration), Phys. Lett. B **241**, 278 (1990).
[43] W. Verkerke and D. Kirkby, *eConf No.* C0303241, MOLT007 (2003) [arXiv:physics/0306116].
[44] https://root.cern.ch/doc/master/classRooNDKeysPdf.html.
[45] M. Ablikim *et al.* (BESIII Collaboration), Phys. Rev. D **94**, 032001 (2016).
[46] $\mathcal{B}_{K_1\to K^-\pi^+\pi^0} = \frac{2}{3}\times\mathcal{B}_{K_1\to K\rho} + \frac{4}{9}\times\mathcal{B}_{K_1\to K^*(892)\pi} + \frac{4}{9}\times 0.93\times \mathcal{B}_{K_1\to K_0^*(1430)\pi}$, where K_1 denotes $\bar{K}_1(1270)^0$.